JJBS

Volume 15, Number 5, December 2022
ISSN 1995-6673
Pages 813 – 824
https://doi.org/10.54319/jjbs/150510

Jordan Journal of Biological Sciences

Insight Towards Induction of Reproductive-Metabolic Phenotypes of Polycystic Ovarian Syndrome

Shaimaa Nasr Amin [1,2,*] , Fida Asali[3,] Mohamed Fathi Mohamed Elrefai[1,4,] Walaa Bayoumie El Gazzar[1,5], Sherif Ahmed Shaltout[6,7], Dalia Azmy Elberry[2], Samaa Samir Kamar[8,9], Noha Samir Abdel Latif [10], Marwa Nagi Mehesen[10,11], Mai Mohammed Ayoub[1], Khaled Anwer Albakri[12] , Asmaa Mohammed ShamsEldeen[2,13]

[1] Department of Anatomy, Physiology, and Biochemistry, Faculty of Medicine, The Hashemite University, PO Box 330127, Zarqa 13133, Jordan; [2] Department of Medical Physiology, Faculty of Medicine, Cairo University, Cairo, Egypt; [3] Department of Obstetrics and Gynaecology, Faculty of Medicine, The Hashemite University, PO Box 330127, Zarqa 13133, Jordan; [4] Department of Anatomy and Embryology, Faculty of Medicine, Ain Shams University, Cairo, Egypt; [5] Department of Medical Biochemistry and Molecular Biology, Faculty of Medicine, Benha University, Benha, Egypt;[6] Department of Pharmacology, Public Health and Clinical skills, The Hashemite University, PO Box 330127, Zarqa 13133, Jordan; [7] Department of Pharmacology, Faculty of Medicine, Benha University, Benha, Egypt;[8] Department of Histology, Faculty of Medicine, Cairo University, Egypt; [9] Department of Histology Armed Forces College of Medicine, Egypt; [10]Department of Medical Pharmacology, Faculty of Medicine, Cairo University, Cairo, Egypt;[11] Department of Pharmacy Practice and Clinical Pharmacy, Faculty of Pharmacy, Future University in Egypt, Cairo, Egypt; [12] Faculty of Medicine, The Hashemite University, PO Box 330127, Zarqa 13133; [13]Physiology department, Faculty of medicine, October 6 University,Giza,Egypt

Received: May 11, 2022; Revised: August 18, 2022; Accepted: August 18, 2022

Abstract

Hormonal disturbances, multiple ovarian cysts, and oligo-anovulation are the key features of the polycystic ovarian syndrome (PCOS). Consistently, without a directly hormone-regulated animal model, we developed three phenotypes of PCOS in rats to simulate the reproductive-metabolic disturbances of human PCOS. Twenty-four female Sprague-Dawley rats underwent vaginal smears for two sequential cycles to exclude any PCOS-like rats. Rats were divided into the following groups: healthy control, PCOS induced by a high-fat, high-sugar (HFHS) diet, PCOS induced by HFHS diet +monosodium glutamate (MSG), and PCOS induced by continuous light exposure (L/L). At the end of the study, an abdominal ultrasound revealed multiple ovarian cysts, and a vaginal smear documented the arrest of the estrous cycle. Serum samples showed hyperinsulinemia and hyperandrogenism in all PCOS-induced groups, but with superiority of the L/L group in developing higher insulin levels, insulin resistance, and anti-Müllerian hormone (AMH). Although the frequency of isolated uterine contractions increased in all modeling groups compared to the control, the contraction amplitude was higher in HFHS than in L/L and HFHS-MSG groups. The three animal models manifested the key features of PCOS and symptoms of metabolic syndrome. Disturbed circadian rhythm and HFHS diet are more in line with the increased risk of PCOS.

Keywords: PCOS, Circadian rhythm, HFHS, AMH, Testosterone.

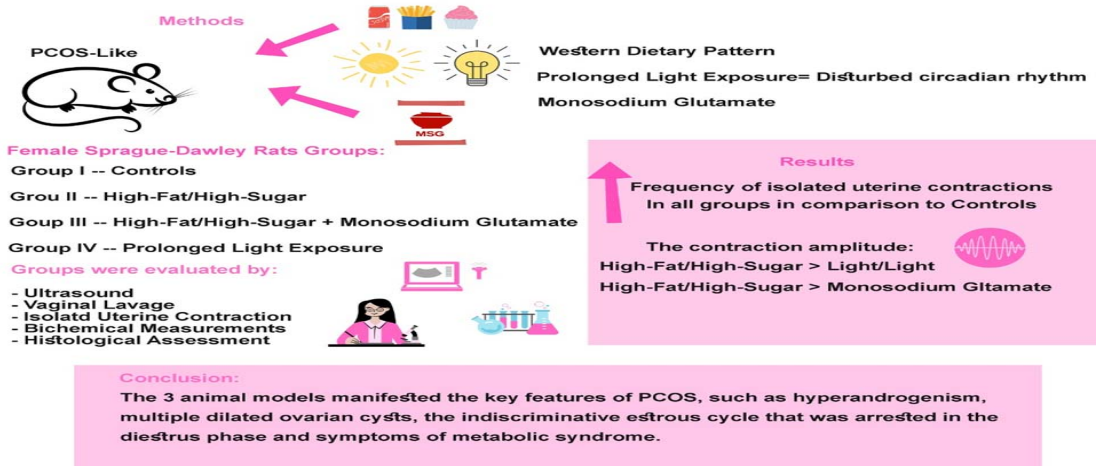

* Corresponding author. e-mail: shaimaa@hu.edu.jo.

1. Introduction

Polycystic ovarian syndrome (PCOS) is the most prevalent metabolic and hormonal dysfunction among reproductive-aged females (Goodarzi et al., 2011) and one of the main contributors to infertility in this age group (Kutcher et al., 2009). It is associated with polycystic ovarian morphology, rarity or lacking ovulation, hyperandrogenism, dyslipidemia, and insulin resistance. The collection of these abnormalities has long-term sequelae like fatty liver, cardiovascular diseases, diabetes, and cancer (Anagnostis et al., 2018).

Although the pathophysiology and etiology of PCOS have not been thoroughly demonstrated, multiple factors can influence women's hormones and metabolic processes during intrauterine and prepuberty life (Anagnostis et al., 2018).

Obesity-induced by diet may contribute to the pathophysiology of PCOS as it causes irregular cycles, hormonal imbalances, and ovarian signaling impairments (Volk et al., 2017). Moreover, the available evidence promotes the importance of substituting diet for pharmacological therapy to alleviate PCOS symptoms and reduce weight and metabolic abnormalities (Toscani et al.,2011).

Almost all food additives function as either palatability enhancers or preservatives. One of these salts is monosodium glutamate (MSG) (Moore, 2003). MSG is a hydrated sodium salt of naturally occurring L-glutamic acid, sold commercially, consisting of glutamate, sodium, contaminants, and water. The harmless endogenously produced glutamate also can be found in natural food, while synthetic glutamate is toxic and found in industrial foods (Chakraborty, 2019). MSG diminishes the functions of the ovary by boosting the production of estradiol, follicle-stimulating hormone (FSH), and luteinizing hormone (LH), which results in enhancing follicular development and oxidative defense (Mondal et al., 2018).

The circadian rhythm allows metabolism to adapt and predict the day's light-dark cycle, ensuring the best physiological functioning. Accordingly, the disruption in this rhythm may lead to several diseases, such as metabolic syndrome and obesity (Moustafa, 2020). On the other hand, PCOS women experience multiple sleep and related psychological problems that decrease sleep quality (Kang et al., 2015). The cyclic light-dark circadian rhythm controls LH surges on which ovulation depends (McCORMACK, 1973). Therefore, any change in these light-dark photoperiods can disturb the normality of the cycle and decrease ovulation, which is a PCOS essential character (Weber and Adler, 1979).

Based on the previous reports on the impact of diet and circadian rhythm disturbances on PCO development, this study aimed to evaluate and compare the impact of diet changes versus circadian rhythm disturbances on ovarian and uterine functions in female rats and correlate the resulting changes to the known picture of PCOS.

2. Materials and Methods

"The Institutional Review Board of The Hashemite University" approved (15/2020) the experimental steps, animal handling, sampling, and euthanasia. The handling of animals followed the "Care and Use of Laboratory Animals guide" (NIH publication no. 85-23, revised 2011).

2.1. A-Experimental design and study groups:

This research followed a randomized controlled animal experimental design including twenty-four female Sprague-Dawley rats whose weight ranged from 150 to 180 g (70 days old). All were subjected to vaginal smears, which were examined by light microscopy for two successive cycles (around 8–10 days), and any PCOS-like rats that showed long estrous cycles (more than 5 days) have been excluded (Hu et al., 2018). The animals were kept in stainless steel cages as three rats per cage to prevent isolation-induced stress, exposed to a 25 °C environmental temperature under a 12:12 h light: dark cycle except for group IV, which was exposed to a 12:12 h light: light cycle (continuous illumination). Rats were categorized into four groups:

Group I- healthy control had free access to water, a regular chow diet (7% simple sugars, 3% fat, 50% polysaccharide, 15% protein), and energy of 3.5 kcal/g (Samuelsson et al., 2008).

Group II-PCOS induced by a high-fat, high-sugar (HFHS) diet had free access to water, a 32% sucrose solution, and high-fat chow (5.24 kcal/g, 60% of calories derived from fat) for 14 weeks (Volk et al., 2017, Nurullahoglu-Atalik et al., 2020).

Group III-PCOS induced by HFHS diet +monosodium glutamate (MSG) had a similar diet to the previous group in addition to MSG daily 0.8 gm/kg BW/day orally by gavage (Mondal et al., 2018) for 14 weeks.

Group IV-PCOS induced by prolonged light exposure were kept in the light experiment box where they were subjected to a continuously illuminated environment (L/L, lights for 24 hours/day) for 14 weeks. The dimensions of the light experiment box were 120 cm in length, 45 cm in width, and 180 cm in height. Furthermore, it is vertically divided into four equal and separated compartments (length, width, and height of 120 cm, 45 cm, and 45 cm per compartment). Each compartment has its ventilation and fluorescent lamp (color temperature: 6500 k, illumination: 600 lux) (Kang et al., 2015).

At week fourteen of the study, an ultrasound was performed to assess ovarian size. Then cervical dislocation was used to euthanize rats. Abdomens were dissected, and blood samples were obtained from the aorta for measurement of serum LH; FSH; Anti-Müllerian Hormone (AMH); Testosterone (T), glucose, insulin, triglycerides (TG); Total Cholesterol (TC); High-density lipoprotein (HDL); Low-density lipoprotein (LDL).

Ovaries were dissected and weighed, then prepared for histopathological examination. The uterus has been separated from all surrounding fat and connective tissue and dissected into two parts; the first recording isolated contractions by Powerlab, and the second was fixed for histopathological examination.

2.2. B-Estrus cycle monitoring:

Vaginal lavage was done daily during weeks 8 to 14 of the study, identifying stages of the estrous cycle through cytological examination. The vaginal cells were flushed with a small amount of distilled water or saline through a

pipette. Then few drops of cell suspension were spread on a glass slide for microscopic examination, allowed to air dry, and subsequently stained with crystal violet stain (McLean et al., 2012).

2.3. C-Abdominal Ultrasound:

Prior to the imaging study, anesthetizing of the rats was done by administration of combined ketamine (100 mg/kg) and xylazine (10 mg/kg) intraperitoneally (Wellington et al., 2013). The fur was removed from the costal margin to the caudal abdomen; next, the anesthetized rat was placed supine on a warmed table to keep the rat safe and comfortable. We used Edan DUS 60 ultrasound diagnostic system with a linear transducer (8.5 MHz) (CA, USA). Female rat ovaries are in fat pads at the end of the uterine horn, lateral to the kidneys bilaterally. (Wang et al., 2017). Ovaries were first measured in the largest sagittal plane as the longest possible diameter (D1) and the second-longest possible ovarian diameter (D2**)** at a right angle to the first measurement. Finally, the mean ovarian diameter (MOD) was calculated using a two-dimensional formula to evaluate ovarian size (Vladimir et al., 2004):

$$MOD = [\{MOD_{\text{left ov.}} = (D1 + D2)/2\} + \{MOD_{\text{right ov.}} = (D1 + D2)/2\}]/2.$$

2.4. D-Isolated Uterine contractions:

The right uterine horn was excised and sliced into longitudinal strips of 5 mm length to record uterine contractility. Each strip was placed vertically in an organ bath containing about 10ml of Krebs–Heinseleit (KH) buffer composed of (mM): NaCl 115.0; KCl 4.6; CaCl2.2H2O 2.5; KH2PO4 1.2; MgSO4.7H2O 2.5; NaHCO3 25 and glucose 11.0 at 37 °C, ventilated with 95% O2/ 5% CO2 throughout the experimental period and solution was replaced every 15 minutes (Darios et al., 2012).

The uterine contractions' changes in isometric force, including amplitude, frequency, and rhythmicity, were recorded using an isometric transducer (Lab Chart software, AD instruments, power lab, New South Wales, Australia). One gm of resting tension was applied first, and the strips were allowed to equilibrate for 60 minutes (Sajadi et al., 2018). Then, recording a 10 min continuous curve was done.

2.5. E-Biochemical measurements & calculations:

Blood samples were left for two hours at room temperature to clot, centrifuged for 10 minutes (4°C) at 1000×g; then serum samples were collected and kept at -20°C till further assessment of the following parameters as per manufacturer's guidelines (MyBioSource, San Diego, CA, USA). Rat ELISA Kits were used for the measurement of serum LH (Catalog No: MBS764675), FSH (Catalog No: MBS2502190), AMH (Catalog No: MBS701712), and Testosterone (Catalog No: MBS282195). Quantitative insulin and fasting serum glucose were measured using Rat Insulin ELISA Kit (Catalog No: MBS045315), and Rat glucose ELISA Kit (Catalog No: MBS7233226) purchased from MyBioSource, San Diego, CA, USA.

The following formula was used to calculate the homeostasis model assessment-estimated insulin resistance (HOMA-IR) index; (HOMA-IR): HOMA−IR = Fasting insulin (μU/mL) × fasting glucose (mmol/L)/22.

Rat Total Cholesterol ELISA Kit (Catalog No: MBS722885), Rat Triglyceride ELISA Kit (Catalog No: MBS726298), and Rat HDL ELISA Kit (Catalog No: MBS704516) purchased from MyBioSource, San Diego, CA, USA was used for Serum total cholesterol (TC), triglycerides (TG) and HDL levels, respectively. Low-density lipoprotein cholesterol (LDLc) levels were estimated using the Friedewald formula: LDL = TC – TG/5 – HDL (Friedewald et al., 1972).

2.6. F-Histological study:

At the end of the experiment, uterine and ovarian tissues were retrieved, fixed in 10% formol saline, processed into paraffin blocks, and seven um serial sections were cut and put on glass slides. Haematoxylin and Eosin were used to stain the sections. (Kiernan, 2001)**.**

2.7. G-Statistical analysis:

Data were analyzed by "SPSS 21" (IBM SPSS Statistics 21; IBM Corporation, New York, USA) and expressed as mean ± standard deviation (Mean ± SD). Normality of distribution was evaluated by Shapiro-Wilk's test. Quantitative variables between the groups were compared using analysis of variance (ANOVA) with the Bonferroni post hoc test. Results were statistically significant at $p \leq 0.05$ (Chan, 2003).

3. Results

3.1. A-Changes in body weight in all studied groups:

There is no significant difference among the rats of the four studied groups at the beginning of the study, as shown in Table 1. However, by the end of the work, there was a significant increase (P-value ≤0.05) in body weight in groups fed on HFHS and HFHS+MSG compared to the control group, while the difference between the L/L group and the control group remained insignificant. The % change in body weight was significantly greater in groups fed on HFHS and HFHS +MSG (26.4% and 28.184%, respectively) compared to the control group and L/L group (12.7% and 13.22%, respectively).

Table 1. Bodyweight and ovarian weight in the studied groups:

	CONTROL	HFHS	HFHS+MSG	L/L
BW1(gm)	146±8.170	146.330±10.230	150.830±14.280	157.500± 8.800
BW2(gm)	164.600±15.380	185±8.366 [a]	193.340±10.320 [a]	178.330±7.500
% Change of Bodyweight	12.700%	26.400%	28.184%	13.220%
Absolute Ovarian weight (mg)	53±8	125±20 [a]	160±32 [a b]	140±7 [a]
Relative Ovarian Weight (*Ovarian Weight / 100 gm of final body weight)* (mg%)	32.3±5.2	67.56±2.4 [a]	82.9±22.2 [a b]	78.5±9.3 [a]

HFHS: High Fat High Sugar; **MSG:** Monosodium Glutamate**; L/L:** Light/Light cycle, **BW1:** Body Weight at the start of the work, **BW2:** Body Wight at the end of the work.

[a]: Significant compared to control group, [b:] significant compared to HFHS group, [c:] significant compared to HFHS+MSG group at P-value≤0.05.

3.2. B- Comparison of ovarian weight and diameter in all groups:

Table 1 shows a significant increase (P-value ≤0.05) of absolute and relative ovarian weight in HFHS, HFHS+MSG, and L/L groups in comparison with the control group, noting that this ovarian weight is significantly higher (P-value ≤0.05) in HFHS+MSG fed group compared to the group fed on HFHS only. As shown in (figure 1), the abdominal Ultrasound revealed a significant expansion (P-value ≤0.05) in the *mean ovarian diameter* in HFHS, HFHS+MSG, L/L groups compared to the control group.

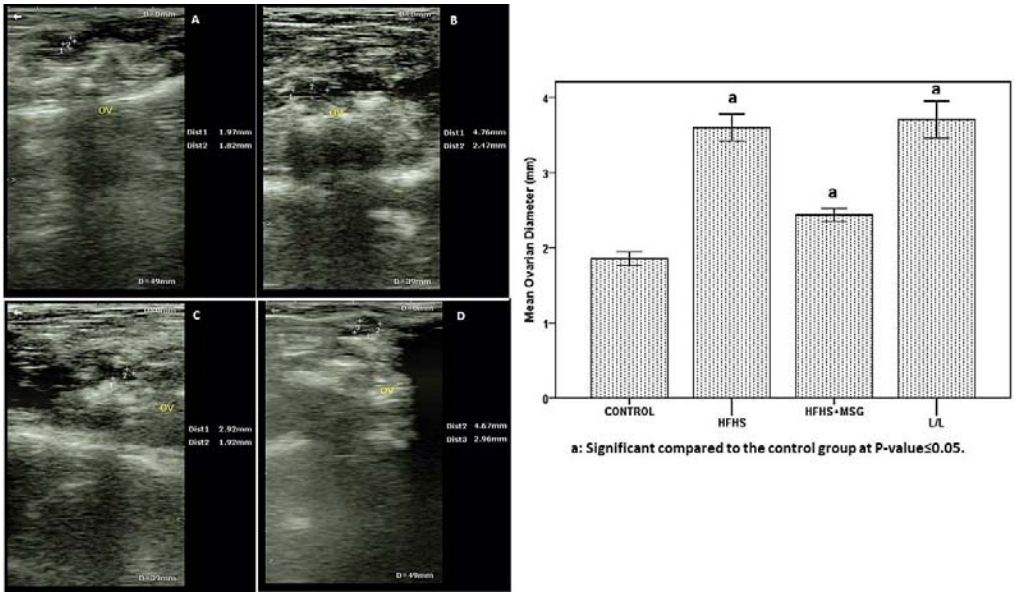

Figure 1. Mean Ovarian Diameter in the studied groups in abdominal Ultrasound. Abdominal Ultrasound: the longest possible diameter (D1) and the second-longest possible ovarian diameter (D2) to be at a right angle to the first measurement.

The mean ovarian diameter (MOD) = [{MOD $_{\text{left ov.}}$ = (D1 + D2)/2} + {MOD $_{\text{right ov.}}$ = (D1 + D2)/2}]/2.

[A: Control group; B: PCO group induced by HFHS; C: PCO group induced by HFHS+MSG; D: PCO group induced by L/L]

3.3. C-Functional assessment of isolated uterine Contractions:

-As shown in **(**table 2) and (figure 2): there is a significant rise (P-value ≤0.05) in the frequency of isolated uterine contractions in HFHS, HFHS+MSG, L/L rats in comparison with the control rats, with its value significantly exceeding (P-value ≤0.05) those in the HFHS+MSG and L/L groups compared to the HFHS group and also significantly higher (P-value ≤0.05) in the L/L group compared to HFHS+MSG group.

While the amplitude of isolated uterine contractions increased significantly in HFHS and L/L groups compared to the control group, its value is significantly lower in the L/L group than in the HFHS group (the highest amplitude recorded). On the other hand, the HFHS+MSG group revealed a significant reduction (P-value ≤0.05) in the contraction amplitude compared with the other three groups. Moreover, figure 2 demonstrated irregular contractions in the HFHS+MSG group compared to the regular contractions recorded in the other three groups.

Table 2. Functional assessment of isolated uterine Contractions in the studied groups:

	CONTROL	HFHS	HFHS+MSG	L/L
Frequency of uterine contractions (contraction/10 minutes)	11.670±1.370	12.330±1.370 [a]	17+.890 [a b]	14.330±.510 [a b c]
The amplitude of uterine contractions (gm tension)	0.490±.030	1.23±.044 [a]	0.160±.030 [a b]	0.780±.020 [a b c]

HFHS: High Fat High Sugar; **MSG:** Monosodium Glutamate**; L/L:** Light/Light Cycle

[a]: Significant compared to the control group, [b:] significant compared to HFHS group, [c:] significant compared to HFHS+MSG group at P-value≤0.05.

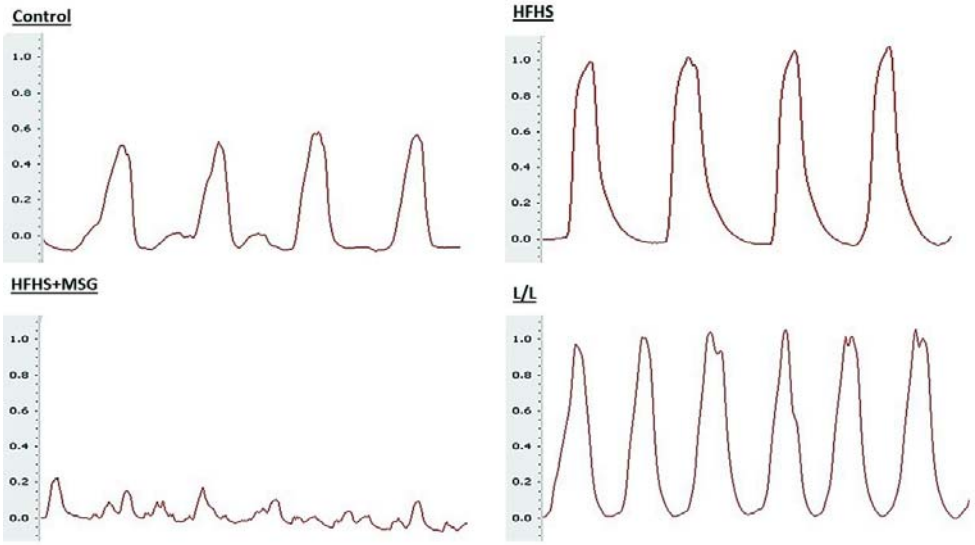

Figure 2. Isolated Uterine Contractions in the studied groups. Increased frequency of isolated uterine contractions in HFHS, HFHS+MSG, L/L groups compared to the control group. The amplitude of isolated uterine contractions increased in HFHS, and L/L groups compared to the control group, noting that its value is lower in the L/L group than in the HFHS group. The HFHS+MSG group showed a decreased contraction amplitude compared to the other three groups with an irregular pattern of contractions.

3.4. D-Biochemical results:

Table 3 shows a significant rise (P-value ≤0.05) in serum levels of LH and Testosterone in HFHS, HFHS+MSG, and L/L groups in comparison with the control group, noting that LH levels are significantly higher (P-value ≤0.05) in the HFHS+MSG group in comparison with the HFHS group. On the contrary, the serum level of FSH decreased significantly (P-value ≤0.05) in HFHS, HFHS+MSG, and L/L groups in comparison with the control group. These findings led to a significant elevation (P-value ≤0.05) in LH/FSH ratio in HFHS, HFHS+MSG, and L/L groups in comparison with the control group, also noting that this ratio is significantly higher (P-value ≤0.05) in the HFHS+MSG and L/L groups in comparison with the HFHS group.

AMH was significantly increased (P-value ≤0.05) in HFHS and L/L groups compared to the control group this increase was not significant in HFHS+MSG compared to control, HFHS, L/L groups.

Serum glucose levels and HOMA-IR were significantly increased (P-value ≤0.05) in HFHS, HFHS+MSG, and L/L groups compared to the control group. Serum glucose or HOMA-IR showed no significant difference among the three model groups (HFHS, HFHS+MSG, L/L groups). In comparison, serum insulin level was significantly increased (P-value ≤0.05) only in the L/L group in comparison with the control and the other two model groups (HFHS, HFHS+MSG), among which there is no significant difference in this serum insulin.

There is a significant elevation (P-value ≤0.05) in serum TG and TC in HFHS, HFHS+MSG, and L/L groups compared to the control group. TC only shows a significant rise (P-value ≤0.05) in the HFHS+MSG and L/L groups compared to the HFHS group.

Serum LDL in HFHS+MSG and L/L groups show a significant elevation (P-value ≤0.05) in comparison with the control and HFHS groups, while there is no significant difference in serum HDL among the studied groups.

Table 3. Biochemical Measurements and calculations in the studied groups:

	CONTROL	HFHS	HFHS+MSG	L/L
Serum LH	13.530± .740	17.250±.520 [a]	19.540±1.480 [a b]	18.150±.450 [a]
Serum FSH (MIU/ml)	9.830±.620	6.010±.450 [a]	5.630±.440 [a]	5.100±.610 [a b]
LH: FSH	1.380±.140	2.890±.300 [a]	3.480±.370 [a b]	3.590±.470 [a b]
Serum Testosterone (ng/ml)	6.400±1.120	8.780±1 [a]	8.400±.840 [a]	8.930±.710 [a]
AMH (ng/ml)	10.980±1.020	12.270±.770 [a]	11.230±.810	12.350±.3100 [a]
Serum Glucose (mmol/ml)	5.150±.680	6.850±.500 [a]	7.590±.450 [a]	6.890±.700 [a]
Serum Insulin (UIU/ml)	7.850±.350	8.320±.360	8.580±.500	9.580±.830 [a b c]
HOMA-IR	1.820±.250	2.560±.120 [a]	2.900±.300 [a]	2.960±.540 [a]
Serum TG (mg/dl)	77±5.800	98.170±5.500 [a]	99±2.960 [a]	103.500±4.700 [a]
Serum TC (mg/dl)	146±5.650	166.660±9.400 [a]	178.830±7.270 [a b]	182.300±3.380 [a b]
Serum HDL (mg/dl)	59±5.290	59.500±5.010	58.300±6.500	55.170±2.780
Serum LDL (mg/dl)	73.160±11.920	87.340±11.130	103.600±6.950 [a b]	106.660±3.900 [a b]

HFHS: High Fat High Sugar; **MSG:** Monosodium Glutamate**; L/L:** Light/Light cycle**; LH**: Luteinizing Hormone**; FSH:** Follicle-stimulating hormone**; AMH:** Anti-Müllerian Hormone**; HOMA-IR:** Homeostatic Model Assessment for Insulin Resistance**; HOMA-B**: Homeostasis model assessment of β-cell function**; TG:** Triglycerides**; TC:** Total Cholesterol**; HDL:** High-density lipoprotein**; LDL:** Low-density lipoprotein; **S100P:** S100 calcium-binding protein P**; ADAMTS19:** A Disintegrin-Like And Metalloprotease With Thrombospondin Type 1 Motif 19; **FLCs:** Free Light Chains.[a]: Significant compared to control group, [b]: significant compared to HFHS group, [c]: significant compared to HFHS+MSG group at P-value≤0.05.

3.5. E-Histopathological results:

3.5.1. -H&E staining of ovarian and uterine sections:

In Figure 3, ovarian sections in the control group showed typical structures of primordial follicles, follicles at different stages, and corpus luteum. However, the PCO group induced by HFHS exhibited multiple degenerated follicles with desquamated cells in the lumen and multiple dilated cysts lined with flattened cells and multiple atretic follicles. In addition, the PCO group induced by HFHS+MSG revealed multiple dilated cysts lined with flattened cells and degenerated follicles. Moreover, the PCO group induced by L/L showed multiple dilated cysts.

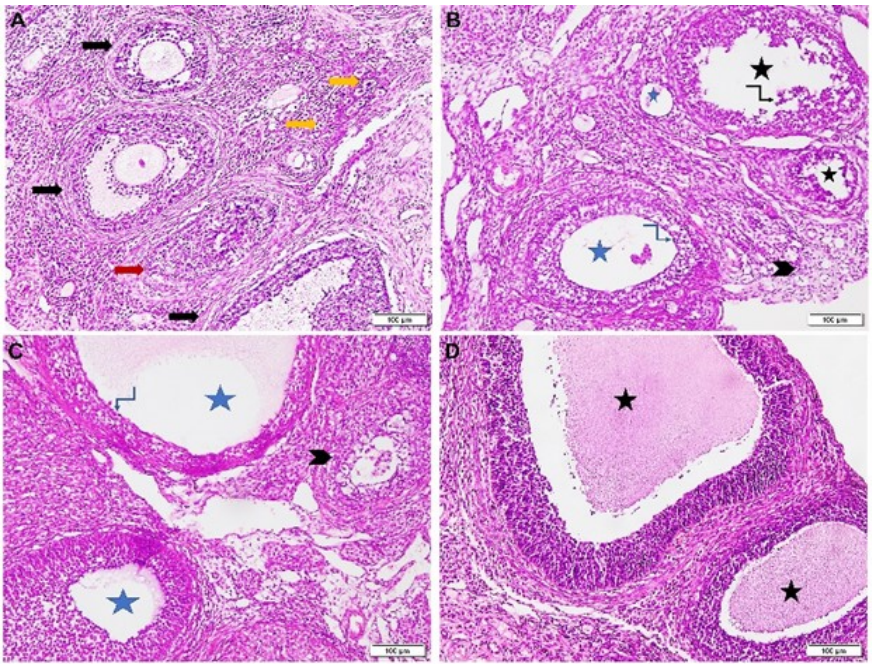

Figure 3: A photomicrograph of sections in the ovary (H&E x100).**A**: Control group showing typical ovarian structure, including primordial follicles (yellow arrows), follicles at different stages (black arrows), and corpus luteum (red arrow).**B**: PCO group induced by HFHS exhibiting multiple degenerated follicles (black asterisk) with desquamated cells in the lumen (kinked arrow) and multiple dilated cysts (blue asterisk) lined with flattened cells (blue kinked arrow) and multiple atretic follicles (arrowhead).**C**: PCO group induced by HFHS+MSG revealing multiple dilated cysts (blue asterisk) lined with flattened cells (blue kinked arrow) and degenerated follicle (arrowhead).**D**: PCO group induced by L/L showing multiple dilated cysts (asterisk).

In (Figure 4), the uterine morphology of control rats revealed a typical uterine structure lined with simple columnar epithelium with underlying connective stroma containing uterine glands. In comparison, the PCO group induced by HFHS revealed a uterus lined with stratified columnar epithelium with underlying connective stroma

rich in eosinophils and contains dilated uterine glands. PCO group induced by HFHS+MSG showed hypertrophied elongated columnar epithelium with underlying connective stroma rich in eosinophils, dilated congested blood vessels, and contains hypertrophied uterine glands. PCO group induced by L/L exhibited stratified columnar epithelium with underlying connective stroma rich in eosinophils and dilated congested blood vessels.

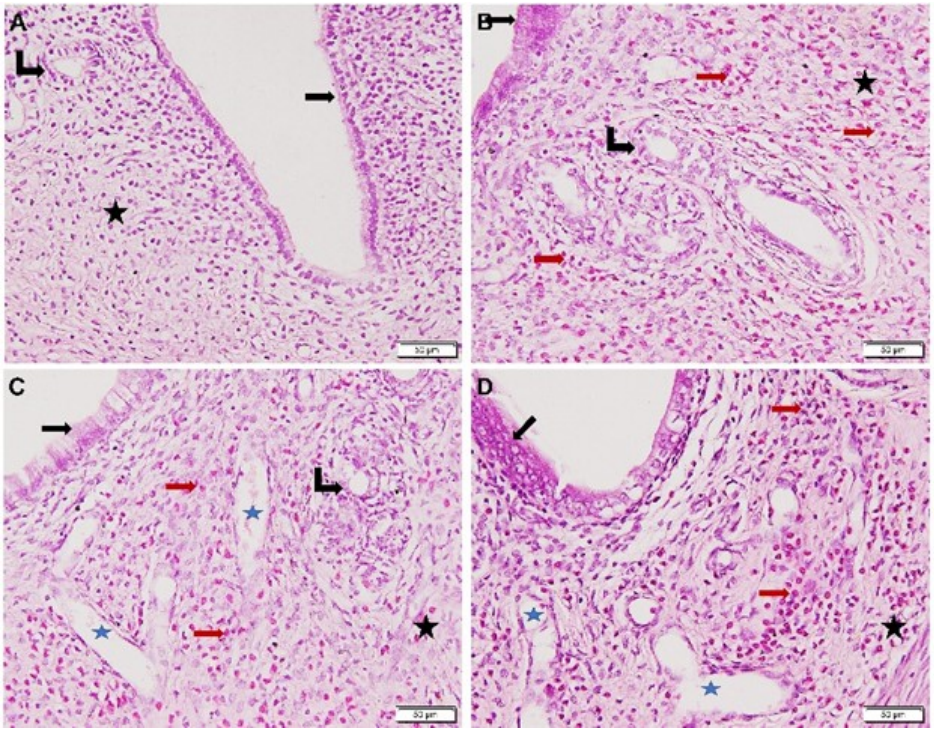

Figure 4. A photomicrograph of uterine sections (H&E x200).**A**: Control group showing typical uterine structure lined with simple columnar epithelium (black arrow) with underlying connective stroma (asterisk) containing uterine glands (kinked arrow).**B**: PCO group induced by HFHS showing uterus lined with stratified columnar epithelium (black arrow) with underlying connective stroma (asterisk) rich in eosinophils (red arrows) and contains dilated uterine glands (kinked arrow).**C**: PCO group induced by HFHS+MSG exhibiting uterine tissue lined with hypertrophied elongated columnar epithelium (black arrow) with underlying connective stroma (asterisk) rich in eosinophils (red arrows), dilated congested blood vessels (blue asterisk), and contains hypertrophied uterine glands (kinked arrow).**D**: PCO group induced by L/L revealing uterus lined with stratified columnar epithelium (black arrow) with underlying connective stroma (asterisk) rich in eosinophils (red arrows) and dilated congested blood vessels (blue asterisk).

Estrus cycle phases in studied groups evaluated by vaginal smear as shown in (figure 5); the vaginal smear of the control group revealed a regular estrus cycle formed of four phases: proestrus, estrus, metestrus, and diestrus. The proestrus phase is characterized by clusters of small, rounded, nucleated cells with central rounded nuclei. The Estrus phase exhibited clusters of cornified non-nucleated squamous epithelial cells. Many cornified epithelial cells with a few darkly stained leucocytes were observed during the metestrus phase. However, the darkly stained leucocytes predominated with few cornified epithelial cells in the diestrus phase, and rarely nucleated cells could be seen. In the PCO group**s** (induced by HFHS, HFHS+MSG, and L/L), the estrus cycle was delayed, and most rats remained in the diestrus phase.

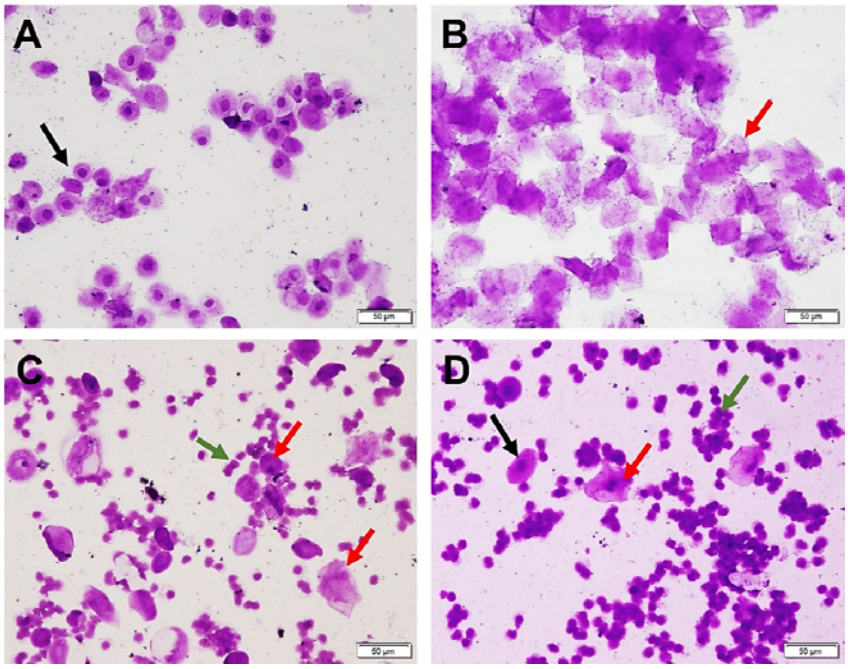

Figure 5. A photomicrograph of vaginal smear showing the different stages of the estrus cycle.

A) Proestrus phase exhibits small, rounded, nucleated cells with central rounded nuclei (black arrow).

B) Estrus phase showing clusters of cornified non-nucleated squamous epithelial cells (red arrow).

C) Metestrus phase reveals a large number of cornified epithelial cells (red arrows) with few darkly stained leucocytes (green arrow).

D) Diestrus phase showing darkly stained leucocytes (green arrow) with few cornified epithelial cells (red arrow). NB, one nucleated cell (black arrow) can be seen.

4. Discussion

Many studies have demonstrated that genetic anomalies, lifestyle, hormonal imbalance before birth, and other environmental causes may give rise to PCOS (Wen et al., 2020). The current study compared the functional, biochemical, and morphological changes in response to dietary changes and circadian rhythm disturbance via continuous light exposure and loss of the normal light-dark cycles.

In the present study, the estrus cycle was delayed in the model groups (induced by HFHS, HFHS+MSG, and L/L), and most rats remained in the diestrus phase. Roberts et al. (2017) showed reproductive abnormalities in HFHS animals. The distribution of estrous cycles varied in a fraction of the time terms spent in proestrus, estrus, and diestrus (Volk et al., 2017).

Previous studies demonstrated that HFHS-fed animals had disrupted estrous cyclicity, with a shorter period in proestrus and longer in estrus than in the controls. A more significant fraction of time recognized in estrus is accompanied by ovulation failure and infertility (Brawer et al., 1986). Another study showed that in MSG treated group, the vaginal mucosa was lined with vacuolated or pyknotic cells with infiltration of leukocytes, and this demonstrates the estrus cycle disturbance in PCO groups induced by MSG (El-Beltagy and Elghaweet, 2016).

Prolonged light exposure can also disturb the estrus cycle in female rats and explain one of the PCO induction theories in females. Kang et al. (2015) reported an indiscriminative estrous cycle in two-thirds of female rats 4 weeks after continuous light exposure and in all L/L rats following 16 weeks of continuous exposure to light, confirmed by daily vaginal smears.

Several studies showed that high-fat, high-sucrose diet rats revealed hyperphagia, rapidly developing obesity, and impaired glucose tolerance (la Fleur et al., 2011; Apolzan and Harris, 2012). That was in accordance with changes in body weight in HFHS and HFHS+MSG compared to the control group.

One environmental factor contributing to PCOS is circadian rhythm disruption (Farhud and Aryan, 2018). Some studies have demonstrated that females subjected to night-light shifts showed irregularity in their menstrual cycles, dysmenorrhea, insulin resistance, and glucose metabolism dysregulation, all of which are recognized risk factors for PCOS (Lim et al., 2018). The continuous light exposure was evidenced to produce PCOS changes and high androgen secretion in rodents (Kang et al., 2017, Chu et al., 2020), which is concomitant with our results.

Besides increased body weight, the present work showed that absolute and relative ovarian weights remarkably increased in rats fed on HFHS and HFHS+MSG compared to the control rats. This is concomitant with Akin tayo et al.'s study (2021), where ovarian weights significantly increased in PCOS animals with or without a fructose-enriched diet. Our results also agree with Hilal et al. (2020), who showed an increase in ovarian weight in mice fed with a HF diet, suggesting that this was due to the rise in their body weights.

Moreover, absolute and relative ovarian weights of rats exposed to L/L environment increased significantly without a significant rise in body weight. This partially

follows Kang et al.'s (2015) study, which revealed ovarian and uterine enlargement associated with weight loss in female rats exposed to continuous light. A significant rise in mean values of ovarian diameter calculated by the abdominal Ultrasound in all PCOS phenotypes was documented compared to the control group. In agreement with our results, enlarged ovaries are also observed in Kang et al.'s study (2015); the authors reported this observation in the L/L group of PCOS in rats induced by a continuous light environment. Another study observed no remarkable rise in the total ovarian volume. However, there was a significant elevation in ratios of volume of the cortex to the medulla volume in the ovaries of HFD mice, suggesting a rise in the number and diameters of cortical follicles (Hilal et al., 2020).

We also noted a significant rise in the frequency and amplitude of the regularity of uterine contractions in HFHS and L/L groups compared to the control. The significant frequency increase was accompanied by a remarkable reduction of amplitude and irregularity of contraction in the HFHS+MSG group compared with the control. Aktas et al. (2019) showed that uterine contractile responses in PCOS showed a significant rise compared to the control group and explained increased myometrium thickness. Another research has demonstrated uterine contractions' irregularities with variant mechanical responses of isolated uteri in PCOS rats (Sajadi et al., 2018).

Other researchers have demonstrated a remarkable increase in myometrium thickness and myometrium area in hyperandrogenised rats (Bracho et al., 2019). Moreover, Sajadi et al. (2018) reported more irregularity in uterine contractions of PCOS rats than in control rats following administration of carbachol and oxytocin.

It is known that preovulation surge needs estradiol's positive feedback that induces kisspeptin expression. Hypothalamus' kisspeptin neurons that project directly to the gonadotropin-releasing hormone may be the feedback mediators. However, it was reported that a fat diet decreased the kisspeptin expression, and decreased sensitivity between the feedback and kisspeptin is also correlated with reduced LH (Zhou et al., 2014). Additionally, HFHS rats show higher estradiol concentrations at proestrus, which may correlate with LH levels' alternation.

Further, saturated fatty acids reduce adenylate cyclase activity, stimulating LH (Cano et al., 2008). This could explain the result of a previous work done by Volk et al. (2017) that showed reduced LH levels at a diestrus among high-fat diet-fed rats compared with those fed a control diet which disagrees with our study. Another study revealed that LH levels have slightly decreased, but there was no significant difference between the two diet patterns (standard and HFHS) (Cano et al., 2008). This disagreement could be explained by the differences in the calories and fats fed to the mice

Moreover, our study revealed a significant increase in anti-Müllerian hormone (AMH) and LH levels in HFHS rats compared to control rats, which is not compatible with the other studies that reported no statistical difference between both diet types (Volk et al., 2017; Roberts et al., 2020). These disagreements could be due to the different sampling times.

The release of the early predictor for ovarian reserve, AMH (Visser et al., 2006), begins after the development from the primordial to the primary follicle. The low FSH reduces this initial recruitment. On the other hand, FSH stimulates the differentiation of antral follicles to reach ovulation requested for cyclic recruitment. Further, AMH may decrease the granulosa cells' receptors of FSH. Accordingly, the absence of AMH increases the number of recruited follicles for growth, which results in depletion of the pool of primordial follicles over time(Roberts et al., 2020).

Continuous light exposure could induce AMH elevation. The identical change in AMH level revealed that in the absence of steroid hormone administration, continuous light environment principally participated in AMH increase, and circadian rhythm disturbance might be critical in the pathology of ovulation abnormality in PCOS (Chu et al., 2020). This is also in line with our results. Among PCOS women, there was a positive association between the number of antral follicles and AMH level in serum; thus, elevated serum levels of AMH are used as a diagnostic way in PCOS. These findings indicate the role of AMH in the pathogenesis of PCOS. However, our study reported an insignificant difference between the HFHS+MSG and control groups regarding AMH levels, which is compatible with a previous study conducted by Gaspar et al. (2016). Based on what we mentioned, any factor that can induce AMH elevation may be considered pathogenic and participate in PCOS development. Our result revealed that the L/L cycle group has a higher AMH level than the control group, which agrees with a previous study (Chu et al., 2020).

The result reported by Volk et al. (2017) revealed that T level was higher in the high-fat diet group in comparison with the control group, which is concomitant with our finding. The suggested explanation is that the increased T level is related to elevated LH within the estrus cycle's negative feedback phase. Moreover, insulin signaling abnormality may alternate the basal releasing of hormones.

On the other hand, previous studies reported no statistical difference between the two diet types regarding the free serum T levels (Cano et al., 2008; Roberts et al., 2017). However, one of these studies demonstrated a linear correlation between the T levels and the number of cysts in the ovary of individual rats in the HFHS group (Roberts et al., 2017).

Our results showed that rats fed on MSG manifested elevated LH and androgen levels. These findings agree with the results of Mondal et al. (2018). Their suggested explanation is that MSG can initiate a positive feedback mechanism on the anterior pituitary by increasing LHRH, which augments LH secretion. Creanga et al. (2008) reported that around one-five of serum T level is released by hyperinsulinemia, increasing LH secretion. Previous studies reported that LH and T levels were significantly increased in light-exposed rats (Zhang et al., 2021). The suggested explanation is that prolonged light exposure may decrease melatonin, which functions directly on the hypothalamus cells and reduces the secretion of the gonadal releasing hormone, leading to increased LH and T levels. These findings align with our study results that showed a significant increase in LH and T levels.

In many ways, obesity participates in PCOS development through insulin resistance and producing

Testosterone from androstenedione in the circulation while decreasing gonadotropin secretion (Arner, 2005). Visceral fat significantly contributes to developing PCOS insulin resistance (Rosen and Spiegelman, 2014). Testosterone and a high-calorie diet probably promote visceral fat accumulation and insulin resistance in women by suppressing lipolysis and enhancing lipogenesis (Rosenfield and Ehrmann, 2016). Dunaif et al., 1992 found that most hyperandrogenic women had androgenic ovarian dysfunction that had nothing to do with elevated serum LH or polycystic ovarian morphology.

Hyperinsulinemia enhances LH stimulation of androgen production from ovaries through up-regulating LH-binding sites and promoting androgen secretion in response to LH at the cytochrome $P450C_{17}$ (Rosenfield and Ehrmann, 2016). Thus, all management ways that decrease serum insulin remarkably improve ovulation and hyperandrogenaemia in PCOS (Turkmen et al., 2016). Both significant increases in serum testosterone in the three PCOS groups and significant hyperinsulinism (especially in the L/L group) were demonstrated by our results, which may explain this increase in the mean ovarian diameter.

Animals in all groups had significantly higher blood glucose levels and showed insulin resistance, as concluded by their high HOMA-IR scores compared to controls. Our results support what was previously reported by Roberts et al., 2017 who demonstrated that animals in the HFHS group had more glucose levels than controls and exhibited insulin resistance.

Our current study also revealed that a continuous light environment caused a significant rise in fasting insulin and glucose levels with elevated HOMA-IR scores. Albreiki et al., (2017) demonstrated that bright light at night was accompanied by a marked increase in plasma glucose and insulin, suggesting glucose intolerance and insulin insensitivity, concomitant with our results. This finding supports what was previously reported by Skinner et al. (2019), who also reported that the increased blood glucose levels induced by the disrupted light cycle exceeded that of the HFD. They suggested that circadian misalignment negatively affects neuroendocrine regulation of body weight and central regulation of glucose homeostasis.

Assessment of lipid profile in the current work revealed higher TG and total cholesterol in all experimental groups compared to controls. Serum LDL significantly increased in HFHS+MSG and L/L groups compared to the control. These results could be related to the apparent insulin resistance and the development of dyslipidemia in these groups. Insulin resistance could also alter systemic lipid metabolism and the development of dyslipidemia (Ormazabal et al., 2018).

Surprisingly, no significant difference was found in HDL levels in the studied groups. This contradicts the work done by Collison et al. (2009), who demonstrated that MSG significantly elevated serum HDL-C, and several studies have reported that circadian misalignment is accompanied by low HDL-cholesterol levels (Ferraz-Bannitz et al., 2021).

Histologically, our study revealed degenerative follicles with desquamated cells in the lumen and dilated cysts lined with flattened cells, more atretic follicles, and a reduction in the number of CL, indicating ovulatory interruption in the HFHS group (Volk et al., 2017). This also agrees with Roberts et al. (2017), who observed the presence of substantial numbers of follicular cysts in HFHS ovaries and a considerable elevation of cystic counts compared to controls. In addition, Ko et al., 2017 found that changes in ovarian histology indicate that female reproductive function may be changed due to high sugar intake.

Following Eweka et al.'s (2011) study, the extracted ovarian specimens from MSG-treated animals showed hypertrophy of the theca folliculi cells, complete distortion, and destruction of the basement membrane between the theca folliculi from the zona granulosa. Degenerative changes with pyknotic nuclei and vacuolated cytoplasm were demonstrated in the oocyte and granulosa cells (Ali et al., 2014). Moreover, the higher dose of MSG led to degenerative and atrophic changes in the ovaries with either apoptotic or necrotic cell death (Eweka and Om'Iniabohs, 2007). Our histopathological results in the MSG group also agreed with those of Bojanić et al., 2009 who reported cystic degenerative effects in the ovary with many atretic follicles and no corpora lutea. In the L/L group, increased number of cystic dilated follicles, thickening of the tunica albuginea in many phases, atretic follicles, fewer granular cell layers, and absent layers of oocytes agreed with Kang et al.'s findings (2015).

Compared to control, the PCO group induced by HFHS revealed a uterus lined with stratified columnar epithelium with underlying connective stroma containing dilated uterine glands. O'Connor et al., 1996 demonstrated that hyperplasia was principally demonstrated in the luminal and glandular epithelium of endometrium and myometrium of the HFD group, which agrees with our results. Kayode et al. (2021) recommended that a high-fat diet may induce some bioactive agents that induce endometrial hyperplasia and protect the uterus against elevated levels of hormones, lipids, and oxidative stress.

Currently, the HFHS+MSG group showed uterine hypertrophied changes. The increase in estrogen levels in the MSG-fed animals may indicate an increase in aromatase enzyme activity that turns Testosterone into estradiol, resulting in elevated estradiol synthesis and the related endometrial changes (Ebbeling et al., 2018, El-Beltagy and Elghaweet, 2016).

In conclusion, to study PCOS with laboratory animals, we have conducted three phenotypes of animal models depending on either diet regimens or altered circadian rhythm. Herein, the continuous light exposure simulates the human sleep disorder, and the intake of HFHS diet simulates the western dietary pattern. The three animal models manifested the key features of PCOS, such as hyperandrogenism, multiple dilated ovarian cysts, the indiscriminative estrous cycle that was arrested in the diestrus phase, and symptoms of metabolic syndrome. Disturbed circadian rhythm and HFHS diet are more consistent with an increased risk of PCOS.

Further research is required to investigate the effect of combined intake of HFHS and the external impacts of continuous light environment on the trait of PCOS and evaluate the potential molecular processes underlying the developed phonotype. More cellular investigations are needed with other techniques like immunohistochemistry and ultrastructural description using an electron microscope; these investigations formed the limitations for

the current study that we will try to elucidate in the following parts of our project.

Funding:

This work received funds from The Hashemite University, Jordan (Research ID:59/2020).

Acknowledgement:

We are grateful to Ms. Yasmeen Jamal Alabdallat for her help in the present study.

Conflict of Interest:

The authors declare the absence of any conflicts of interest.

Statement of Data Availability:

On reasonable request, the supporting data of this study's findings can be provided by the corresponding author, [SN. Amin].

References:

Akintayo, C.O., Johnson, A.D., Badejogbin, O.C., Olaniyi, K.S., Oniyide, A.A., Ajadi, I.O., Ojewale, A.O., Adeyomoye, O.I., Kayode, A.B., 2021. High fructose-enriched diet synergistically exacerbates endocrine but not metabolic changes in letrozole-induced polycystic ovarian syndrome in Wistar rats. Heliyon, 7: e05890.

Aktas, S., Un, I., Barlas, I.O., Ozturk, A.B., Karagul, M.I., 2019. Evaluation of the Rho A/Rho-kinase pathway in the uterus of the rat model of polycystic ovary syndrome. Reprod. Biol, 19: 45–54.

Albreiki, M.S., Middleton, B., Hampton, S.M., 2017. A single night light exposure acutely alters hormonal and metabolic responses in healthy participants. Endocr. Connect, 6: 100–110.

Ali AA, El-Seify GH, El Haroun HM, Mohammed Soliman MA.2014. Effect of monosodium glutamate on the ovaries of adult female albino rats and the possible protective role of green tea. Menoufia Med J, 27:793-800

Anagnostis, P., Tarlatzis, B.C., Kauffman, R.P., 2018. Polycystic ovarian syndrome (PCOS): Long-term metabolic consequences. Metabolism, 86: 33–43.

Apolzan, J.W., Harris, R.B. 2012. Differential effects of chow and purified diet on the consumption of sucrose solution and lard and the development of obesity. Physiol. Behav, 105: 325–331.

Arner, P., 2005. Effects of Testosterone on fat cell lipolysis. Species differences and possible role in polycystic ovarian syndrome. Biochimie, 87: 39–43.

Bojanić, V., Bojanić, Z., Najman, Stevo, Savić, T., Jakovljević, V., Najman, Staša, Jančić, S., 2009. Diltiazem prevention of toxic effects of monosodium glutamate on ovaries in rats. Gen Physiol Biophys, 28: 149–154.

Bracho, G.S., Altamirano, G.A., Kass, L., Luque, E.H., Bosquiazzo, V.L. 2019. Hyperandrogenism induces histo-architectural changes in the rat uterus. Reprod. Sci, 26: 657–668.

Brawer, J.R., Munoz, M., Farookhi, R. 1986. Development of the Polycystic Ovarian Condition (PCO) in the Estradiol Valerate-Treated Rat. Biol. Reprod. 35:647–655.

Cano, P., Jiménez-Ortega, V., Larrad, Á., Toso, C.F.R., Cardinali, D.P., Esquifino, A.I. 2008. Effect of a high-fat diet on 24-h pattern of circulating levels of prolactin, luteinizing hormone, Testosterone, corticosterone, thyroid-stimulating hormone and glucose, and pineal melatonin content, in rats. Endocrine, 33: 118–125.

Chakraborty, S.P. 2019. Patho-physiological and toxicological aspects of monosodium glutamate. Toxicol. Mech. Methods. 29: 389–396.

Chan, Y., 2003. **Biostatistics 102**: quantitative data–parametric & non-parametric tests. Blood Press.

Chu, W., Zhai, J., Xu, J., Li, S., Li, W., Chen, Z.-J., Du, Y. 2020. Continuous light-induced PCOS-like changes in reproduction, metabolism, and gut microbiota in Sprague-Dawley rats. Front. Microbiol, 10: 3145.

Collison, K.S., Maqbool, Z., Saleh, S.M., Inglis, A., Makhoul, N.J., Bakheet, R., Al-Johi, M., Al-Rabiah, R., Zaidi, M.Z., Al-Mohanna, F.A. 2009. Effect of dietary monosodium glutamate on trans-fat-induced nonalcoholic fatty liver disease. J. Lipid Res, 50: 1521–1537.

Creanga, A.A., Bradley, H.M., McCormick, C., Witkop, C.T. 2008. Use of metformin in polycystic ovary syndrome: a meta-analysis. Obstet. Gynecol, 111: 959–968.

Darios, E.S., Seitz, B., Watts, S.W. 2012. Smooth muscle pharmacology in the isolated virgin and pregnant rat uterus and cervix. J. Pharmacol. Exp. Ther, 341: 587–596.

Dunaif A, Givens J, Haseltine F, Merriam G, 1992. **Polycystic Ovary Syndrome.** Cambridge, MA: Blackwell Scientific Publications.

Ebbeling, C.B., Feldman, H.A., Klein, G.L., Wong, J.M.W., Bielak, L., Steltz, S.K., Luoto, P.K., Wolfe, R.R., Wong, W.W., Ludwig, D.S. 2018. Effects of a low carbohydrate diet on energy expenditure during weight loss maintenance: randomized trial. BMJ, 363: k4583.

El-Beltagy, A.E.-F.B.M., Elghaweet, H.A. 2016. Adverse effects of monosodium glutamate on the reproductive organs of adult Female albino rats and the possible ameliorated role of carob (Ceratonia Siliqua). J. Biosci. Appl. Res. 2: 170–184.

Eweka, A., Igbigbi, P., Ucheya, R. 2011. Histochemical studies of the effects of monosodium glutamate on the liver of adult Wistar rats. Ann. Med. Health Sci. Res, 1: 21–30.

Eweka, A., Om'Iniabohs, F. 2007. Histological studies of the effects of monosodium glutamate on the small intestine of adult Wistar rat. Electron J Biomed, 2: 14–18.

Farhud, D., Aryan, Z., 2018. Circadian rhythm, lifestyle and health: a narrative review. Iran. J. Public Health, 47: 1068.

Ferraz-Bannitz, R., Beraldo, R.A., Coelho, P.O., Moreira, A.C., Castro, M., Foss-Freitas, M.C. 2021. Circadian Misalignment Induced by Chronic Night Shift Work Promotes Endoplasmic Reticulum Stress Activation Impacting Directly on Human Metabolism. Biology, 10: 197.

Friedewald, W.T., Levy, R.I., Fredrickson, D.S. 1972. Estimation of the concentration of low-density lipoprotein cholesterol in plasma, without use of the preparative ultracentrifuge. Clin. Chem, 18: 499–502.

Gaspar, R.S., Benevides, R., Fontelles, J., Vale, C.C., França, L.M., Barros Pde, T., Paes, A. 2016. Reproductive alterations in hyperinsulinemic but normoandrogenic MSG obese female rats. J Endocrinol, 229: 61–72.

Goodarzi, M.O., Dumesic, D.A., Chazenbalk, G., Azziz, R. 2011. Polycystic ovary syndrome: etiology, pathogenesis and diagnosis. Nat. Rev. Endocrinol, 7: 219–231.

Hilal, G., Fatma, T., Ferruh, Y., Sabire, G., Yüksel, A. 2020. Effect of high-fat diet on the various morphological parameters of the ovary. Anat. Cell Biol, 53:58-67.

Hu, M., Zhang, Y., Feng, J., Xu, X., Zhang, J., Zhao, W., Guo, X., Li, J., Vestin, E., Cui, P. 2018. Uterine progesterone signaling is a target for metformin therapy in PCOS-like rats. J. Endocrinol, 237: 123–137.

Kang, X., Jia, L., Li, Y., Zhang, X., 2017. Acupuncture attenuates hyperglycaemia and improves ovarian function in female rats subjected to continuous light exposure. Acupunct. Med. 35: 352–359.

Kang, X., Jia, L., Shen, X., 2015. Manifestation of hyperandrogenism in the continuous light exposure induced PCOS rat model. BioMed Res. Int. 2015:943694.

Kayode, O., Kayode, A., Mgbojikwe, I., Rotimi, D. 2021. Effect of Ketogenic Diet on Monosodium Glutamate-Induced Uterine Fibroids in Female Wistar Rats. J. Babol Univ. Med. Sci, 23: 1–8.

Kiernan JK. 2001.**Histological and Histochemical Methods. In: Theory and practice. 3rd ed.,** Arnold Publisher, London, New York, and New Delhy.

Ko, E.-A., Kim, H.-R., Kim, Y.-B., Kim, H.-S., Lee, S.-H..2017. Effect of High Fructose Corn Syrup (HFCS) intake on the female reproductive organs and lipid accumulation in adult rats. Dev. Reprod. 21:151-156

la Fleur, S., Luijendijk, M., Van Rozen, A., Kalsbeek, A., Adan, R.2011. A free-choice high-fat high-sugar diet induces glucose intolerance and insulin unresponsiveness to a glucose load not explained by obesity. Int. J. Obes. 35: 595–604.

Lim, Y.C., Hoe, V.C., Darus, A., Bhoo-Pathy, N. 2018. Association between night-shift work, sleep quality and metabolic syndrome. Occup. Environ. Med, 75: 716–723.

McCORMACK, C.E., 1973. Acute Effects of Altered Photoperiods on the Onset of Ovulation in Gonadotropin-Treated Immature Rats. Endocrinology, 93: 403–410.

McLean, A.C., Valenzuela, N., Fai, S., Bennett, S.A. 2012. Performing vaginal lavage, crystal violet staining, and vaginal cytological evaluation for mouse estrous cycle staging identification. JoVE, 15: e4389.

Mondal, M., Sarkar, K., Nath, P.P., Paul, G., 2018. Monosodium glutamate suppresses the female reproductive function by impairing the functions of ovary and uterus in rat. Environ. Toxicol, 33:198–208.

Moore, K., 2003. **Congenital malformations due to environmental factors. 2nd Ed** Saunders, Philadelphia.

Moustafa, A. 2020. Effect of light-dark cycle misalignment on the hypothalamic-pituitary-gonadal axis, testicular oxidative stress, and expression of clock genes in adult male rats. Int. J. Endocrinol, 2020:1426846.

Nurullahoglu-Atalik KE, Yerlikaya Humeyra, Oz Mehmet, Esen Hasan. 2020. Determining the Response to Statins in Rat Aorta Using High Fat Diet.JJBS, 13(1):1-6.

Ormazabal, V., Nair, S., Elfeky, O., Aguayo, C., Salomon, C., Zuñiga, F.A. 2018. Association between insulin resistance and the development of cardiovascular disease. Cardiovasc. Diabetol, 17: 1–14.

Roberts, J.A., Carpenter, R.M., Blythe, S.N., Toporikova, N. 2020. FSH/AMH ratio and adipocyte size are linked to ovarian dysfunction. Endocr. Res, 45: 174–189.

Roberts, J.S., Perets, R.A., Sarfert, K.S., Bowman, J.J., Ozark, P.A., Whitworth, G.B., Blythe, S.N., Toporikova, N. 2017. High-fat high-sugar diet induces polycystic ovary syndrome in a rodent model. Biol. Reprod, 96: 551–562.

Rosen, E.D., Spiegelman, B.M. 2014. What we talk about when we talk about fat. Cell, 156: 20–44.

Rosenfield, R.L., Ehrmann, D.A., 2016. The pathogenesis of polycystic ovary syndrome (PCOS): the hypothesis of PCOS as functional ovarian hyperandrogenism revisited. Endocr. Rev, 37: 467–520.

Sajadi, M., Noroozzadeh, M., Bagheripour, F., Tehrani, F.R. 2018. Contractions in the isolated uterus of a rat model of polycystic ovary syndrome compared to controls in adulthood. Int. J. Endocrinol. Metab, 16: e63135.

Samuelsson, A.-M., Matthews, P.A., Argenton, M., Christie, M.R., McConnell, J.M., Jansen, E.H., Piersma, A.H., Ozanne, S.E., Twinn, D.F., Remacle, C., 2008. Diet-induced obesity in female mice leads to offspring hyperphagia, adiposity, hypertension, and insulin resistance: a novel murine model of developmental programming. Hypertension, 51: 383–392.

Skinner, N.J., Rizwan, M.Z., Grattan, D.R., Tups, A., 2019. Chronic light cycle disruption alters central insulin and leptin signaling as well as metabolic markers in male mice. Endocrinology, 160:2257–2270.

Toscani, M. K., Mario, F. M., Radavelli-Bagatini, S., Wiltgen, D., Matos, M. C., & Spritzer, P. M. 2011. Effect of high-protein or normal-protein diet on weight loss, body composition,hormone, and metabolic profile in southern Brazilian women with polycystic ovary syndrome: a randomized study. Gynecol Endocrinol, 27: 925-930.

Turkmen, S., Ahangari, A., Bäckstrom, T. 2016. Roux-en-Y gastric bypass surgery in patients with polycystic ovary syndrome and metabolic syndrome. Obes. Surg. 26: 111–118.

Visser JA, de Jong FH, Laven JS, Themmen AP.2006. Anti-Müllerian hormone: a new marker for ovarian function. Reproduction, 131:1-9.

Volk, K.M., Pogrebna, V.V., Roberts, J.A., Zachry, J.E., Blythe, S.N., Toporikova, N., 2017. High-fat, high-sugar diet disrupts the preovulatory hormone surge and induces cystic ovaries in cycling female rats. J. Endocr. Soc. 1: 1488–1505.

Wang, T., Oltra-Rodríguez, L., García-Carrillo, N., Nieto, A., Cao, Y., Sánchez-Ferrer, M.L., 2017. Ultrasonography in Experimental Reproductive Investigations on Rats. J Vis Exp. 130:56038.

Weber, A.L., Adler, N.T., 1979. Delay of Constant Light-Induced Persistent Vaginal Estrus by 24-Hour Time Cues in Rats. Science, 204:323-325.

Wellington, D., Mikaelian, I., Singer, L., 2013. Comparison of ketamine–xylazine and ketamine–dexmedetomidine anesthesia and intraperitoneal tolerance in rats. J. Am. Assoc. Lab. Anim. Sci. 52: 481–487.

Wen, L., Liu, Q., Xu, J., Liu, X., Shi, C., Yang, Z., Zhang, Y., Xu, H., Liu, J., Yang, H. 2020. Recent advances in mammalian reproductive biology. Sci. China Life Sci. 63, 18–58.

Zhang, L., Liu, Y., Li, M., Zhu, X., Shi, Y., 2021. Effect of a high-calorie diet and constant light exposure on female reproduction, metabolism and immune inflammation: A comparative study of different mouse models. Am. J. Reprod. Immunol,86: e13479.

Zhou Q, Chen H, Yang S, Li Y, Wang B, Chen Y, Wu X.2014. High-fat diet decreases the expression of Kiss1 mRNA and kisspeptin in the ovary and increases ovulatory dysfunction in postpubertal female rats. Reprod Biol Endocrinol, 12:127.